

# Adhesion Energy, Surface Traction and Surface Tension in Fe-Mg Binary Alloys

Gboyega A. Adebayo<sup>a,b</sup> and Bede C. Anusionwu<sup>a,c</sup>

<sup>a</sup> International Centre for Theoretical Physics, Strada Costiera 11, P.O. Box 586, I-34014 Trieste, Italy

<sup>b</sup> Department of Physics, University of Agriculture, PMB 2240, Abeokuta, Nigeria

<sup>c</sup> Department of Physics, Federal University of Technology, Owerri, Nigeria

Reprint requests to G. A. A.; E-mail: gadebayo@ictp.it

Z. Naturforsch. **62a**, 596–600 (2007); received May 29, 2007

We present adhesion and surface energies of Fe-Mg binary alloys from simulation studies. The adhesion energy was calculated using the assumption that work is done when atoms come into contact by moving two surfaces from equilibrium position  $z_0$  to  $\infty$ , while the surface traction was determined from the atomic interactions between atoms. The surface tension variation with temperature was investigated from the diffusion coefficient obtained by performing molecular dynamics simulations at temperatures above the eutectic temperature of Fe-Mg. It was observed that the structural information as well as the calculated surface tension suggest segregation in Fe-Mg alloys at all investigated temperatures.

*Key words:* Self-Diffusion Coefficient; Binary Alloys; Viscosity; Lennard-Jones Potential.

*PACS numbers:* 61.20.-p, 61.20.Ja.

## 1. Introduction

Thermophysical properties are necessary to understand the hydrodynamic processes in molten binary alloys. In particular, metallurgists are interested in how the temperature affects casting and welding processes. On the geophysics side, magnesiowuestite is the second abundant mineral in the interior of the earth, and it is normal to expect formation of binary complexes at the conditions of the earth's interior. So one of the motivations for this work is the geophysical point of view, especially the thermophysical properties of Fe-Mg alloys.

The magnetic and electromagnetic measurements of Fe-Mg have been carried out by a number of researchers [1–3], yet others have used different methods to determine the solubility of Fe in liquid Mg [4–6], some X-ray measurements of Fe-Mg alloys were carried out by Bulian and Fahrenhorst [3] and also independently by Mitchell [7]. In recent times, thermophysical properties of binary alloys have been carried out among others, by Keene [8], Egry et al. [9], Seyhan and Egry [10], Xiao et al. [11] and by Novakovic and co-workers [12]. We have not found in the literatures any recent work on Fe-Mg alloys, which is a second motivation for the present investigation.

In Section 2 we highlight the theoretical method used in our calculations. In Section 3 we give detailed results and a discussion of the findings of this work, while Section 4 contains the major conclusions.

## 2. Theory and Method of Simulations

A good starting place for any molecular dynamics simulation is the selection of a potential function to mimic the system of interest. Once this has been done, other assumptions can be made depending on what properties are of interest. We have started our simulations by enclosing 320 atoms of Fe and 680 atoms of Mg in a simulation box with periodic boundary conditions. Reduced units were chosen with the eutectic temperature (Mg) of 923 K as unit of temperature. Calculations were done at 1373 K, 1473 K and 1573 K, corresponding to reduced temperatures of 1.4875, 1.5958 and 1.7042, respectively, and at 1273 K.

After a potential has been chosen, atoms were assigned an initial configuration of positions and velocities, accordingly. Potential and forces on atoms were calculated at each time step. This procedure consists of solving numerical equations of atomic motion using Newton's second law. The mass of an atom was set to

unity for convenience, while interactions beyond the cut-off radius distance  $r_c = \frac{1}{2}L$  were set to zero, and correction terms were added where needed.  $L$  is the simulation box length. Integration of the equation of motion was performed using the Verlet algorithm [13]. Each run was carried out over 15 ps. The pairwise potential used in the present work is the Lennard-Jones (LJ) 12-6 potential given by

$$V(r) = 4\varepsilon_{\text{Fe-Mg}} \left[ \left( \frac{\sigma_{\text{Fe-Mg}}}{r} \right)^{12} - \left( \frac{\sigma_{\text{Fe-Mg}}}{r} \right)^6 \right], \quad (1)$$

where  $\varepsilon_{\text{Fe-Mg}}$  is a parameter determining the depth of the potential well or the bond energy and  $\sigma_{\text{Fe-Mg}}$  is the length scale parameter that determines the position of the potential minimum. We have determined  $\varepsilon$  and  $\sigma$  using the product and additive rules [14]:

$$\varepsilon_{\text{Fe-Mg}} = \sqrt{\varepsilon_{\text{Fe}}\varepsilon_{\text{Mg}}} \quad \text{and} \quad \sigma_{\text{Fe-Mg}} = \frac{\sigma_{\text{Fe}} + \sigma_{\text{Mg}}}{2}. \quad (2)$$

The parameters  $\varepsilon_i$  and  $\sigma_i$  were obtained based on the total energy [15] of a crystal

$$\Phi = \frac{1}{2}4N\varepsilon \left[ \sum_j \left( \frac{\sigma}{\rho_{ij}r_N} \right)^{12} - \sum_j \left( \frac{\sigma}{\rho_{ij}r_N} \right)^6 \right], \quad (3)$$

and it should be noticed that  $\rho_{ij}r_N$  is the distance between a reference atom  $i$  and another atom  $j$  in terms of the distance of the nearest neighbour. Also, we note that the nearest neighbours will contribute most of this interaction energy, so that we can actually say:

$$\Phi = \frac{1}{2}4N\varepsilon C_n \left[ \left( \frac{\sigma}{r_N} \right)^{12} - \left( \frac{\sigma}{r_N} \right)^6 \right], \quad (4)$$

where  $N$  is the total number of atoms in a system and  $C_n$  is the coordination number. The equilibrium  $r_N$  for the minimum total energy with respect to the coordination number will then be

$$\frac{d\Phi}{dr_N} = 0, \quad (5)$$

so that

$$\sigma = r_N 2^{-\frac{1}{6}}. \quad (6)$$

The force of attraction between two atoms may be written as

$$F = -\frac{dV(r)}{dr} = -24\varepsilon_{\text{Fe-Mg}} \left[ \frac{\sigma_{\text{Fe-Mg}}^6}{r^7} - \frac{2\sigma_{\text{Fe-Mg}}^{12}}{r^{13}} \right]. \quad (7)$$

In macroscopic systems, we can represent the atomic interactions between atoms by surface tractions [16] and by assuming the surface traction to be in the  $z$ -direction, then for an LJ potential one can write the surface traction [17]

$$\begin{aligned} T_0(z) &= \frac{A}{6\pi z_0^3} \left[ \left( \frac{z_0}{z} \right)^3 - \left( \frac{z_0}{z} \right)^9 \right] \\ &= \frac{8\Delta\gamma}{3z_0} \left[ \left( \frac{z_0}{z} \right)^3 - \left( \frac{z_0}{z} \right)^9 \right], \end{aligned} \quad (8)$$

where  $A$  is known as the Hamakar constant [18] and is defined as

$$A = 4\varepsilon\pi^2\rho_1\rho_2\sigma^6, \quad (9)$$

where  $\rho_1$  and  $\rho_2$  are the densities of the atoms in contact. The surfaces of the two atoms are in equilibrium when  $T_0 = 0$ , which means the equilibrium distance  $z_0$  is written as

$$z_0 = \left( \frac{2}{15} \right)^{\frac{1}{6}} \sigma. \quad (10)$$

We can now define  $\Delta\gamma$  as the adhesion energy between the surface of two atoms in contact, which is the work done to move two surfaces from equilibrium separation  $z_0$  to infinity:

$$\Delta\gamma = \int_{z_0}^{\infty} T_0(z)dz = \frac{A}{16\pi z_0^2}. \quad (11)$$

Both the liquid-vapour surface tension  $\beta_{\text{lv}}$  and viscosity  $\eta$  are related by the equation [19]

$$\begin{aligned} \eta(T) &= \frac{16\beta_{\text{lv}}(T)}{15} \sqrt{\frac{M}{N_A k_B T}} \\ &= \frac{16}{15} \beta_{\text{lv}}(T) \sqrt{\frac{m}{k_B T}}, \end{aligned} \quad (12)$$

or by the diffusion coefficient

$$D(T) = \frac{5 k_B T}{32\pi r \beta_{\text{lv}}(T)} \sqrt{\frac{N_A k_B T}{M}}, \quad (13)$$

where  $N_A$ ,  $M$  and  $k_B$  are, respectively, the Avogadro's number, atomic mass and Boltzmann's constant. The above equation then allows to determine the surface tension as function of the temperature. The equation above was fitted to

$$\beta_{\text{lv}}(T) = \beta_1^0 + k(T - T_e). \quad (14)$$

Here,  $\beta_1^0$  is the surface tension at the eutectic temperature ( $T_e$ ), and  $k$  is the temperature coefficient of surface tension  $\frac{\partial \beta_{1v}}{\partial T}$ . The appropriate fit is of the form

$$\beta_{1v} = 0.012774 + 5.538e - 5T', \quad (15)$$

where  $T' = (T - T_e)$ , and if we compare this with Butler's [20] equation, we have

$$\beta_{1v} = \beta_1 + \frac{\mu_1^i - \mu_1^B}{A^1} = \beta_2 + \frac{\mu_2^i - \mu_2^B}{A^2}. \quad (16)$$

At equilibrium, one expects  $\beta_1^0 = \beta_1 = \beta_2$ , so that we can say:

$$k(T - T_e) \equiv \frac{\mu_1^i - \mu_1^B}{A^1} = \frac{\mu_2^i - \mu_2^B}{A^2}, \quad (17)$$

where  $\mu_j^i$ ,  $\mu_j^B$  and  $A^j$  are the chemical potentials at the interface, bulk and the area of the species  $j$ , respectively. If we define

$$\Delta\mu_j = \mu_j^i - \mu_j^B \quad (18)$$

as the change in the chemical potential at the point of contact between the species (interface), then

$$\Delta\mu_j = A^j 5.538e - 5T' \quad (19)$$

and

$$A^j = \pi r_j^2. \quad (20)$$

Here  $r_j$  is the atomic radius of the species  $j$ .

### 3. Results and Discussion

The input parameters of the Lennard-Jones potential used in the present work are given in Table 1. They have been chosen as stated above.

The above equations suggest that in Fe-Mg the product of  $5.538e - 5$  and the atomic area  $A^j$  of a species gives the slope of the  $\Delta\mu_j$  vs.  $T'$  curve. The calculated adhesion energy for Fe-Mg was  $2.1981 \text{ J/m}^2$ . Figure 1 shows the curve of the surface traction in Fe-Mg with a peak occurring at  $z = 2.24 \text{ \AA}$ . From the plot it is seen that the attractive force between two (spherical) surfaces has a constant value at a gap less than a certain separation and goes to zero at large separations. If we use the Maugis theory [21], we see that a dimensionless parameter

$$\mathcal{A} = 1.03 \frac{\Delta\gamma}{z_o} \left( \frac{9R}{2\pi\Delta\gamma\mathcal{E}^2} \right)^{\frac{1}{3}} \quad (21)$$

Table 1. Parameters of the Lennard-Jones potential as used in the present calculations.

	$\epsilon$ (eV)	$\sigma$ ( $\text{\AA}$ )
Fe	0.5264	2.3210
Mg	0.0958	2.8800
Fe-Mg	0.2245	2.6005

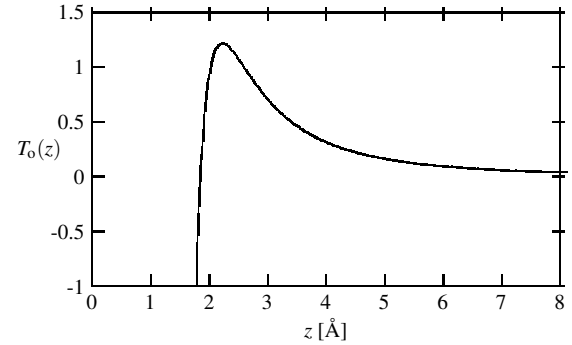


Fig. 1. Atomic interactions between atoms in Fe-Mg alloy.

allows to comment on the effective elastic modulus  $\mathcal{E}$  of the constituent species:

$$\mathcal{E} = \sqrt{\left( \frac{1.03\Delta\gamma}{z_o\mathcal{A}} \right)^{\frac{1}{3}}} \sqrt{\frac{9R}{2\pi\Delta\gamma}}, \quad (22)$$

where  $R = \frac{\sigma_1\sigma_2}{2(\sigma_1+\sigma_2)}$  is the contact radius. It is worth mentioning that  $\mathcal{A}$  can be seen as a measure of the ratio of elastic deformation to the effective range over which the surface traction is valid. We also note that  $\mathcal{E}$  can be written in terms of the Poisson ratio  $\mathcal{P}_i$  and Young's modulus  $\mathcal{Y}_i$  of the species:

$$\mathcal{E} = \left( \frac{1 - \mathcal{P}_1}{\mathcal{Y}_1} + \frac{1 - \mathcal{P}_2}{\mathcal{Y}_2} \right)^{-1}. \quad (23)$$

Figure 2 shows the relationship between the effective elastic modulus  $\mathcal{E}$  and  $\mathcal{A}$ . The effective elastic modulus decreases as  $\mathcal{A}$  increases. At equilibrium, using the contact radius  $R$ , the calculated effective elastic modulus is  $142.9 \text{ GPa}$ . Figure 3 shows the plot of  $\Delta\mu_j$  against  $T'$ , the crosses represent Mg, while the diamonds are the plots of Fe.

A second look at Fig. 3 will suggest that if one looks at the surface free energy as a function of temperature, this will largely be dominated by the surface layer and not by subsurface layers of pure Mg. This is because Mg has a higher  $\Delta\mu$  suggesting higher surface energy than in Fe.

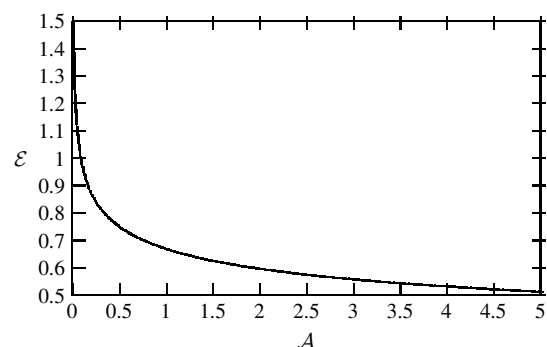


Fig. 2. Variation of the effective elastic modulus  $\mathcal{E}$  of the Fe-Mg alloy as a function of  $\mathcal{A}$ .

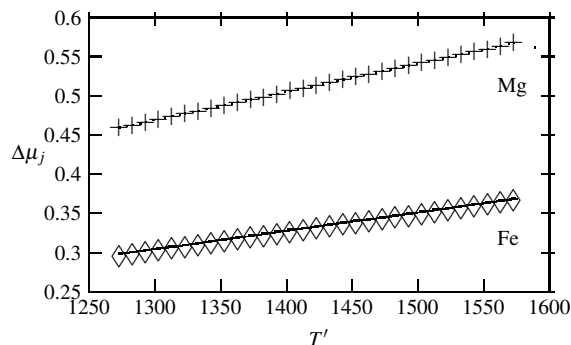


Fig. 3. Change in the chemical potential between the interface and bulk.

In Table 2, we present the structural information from our calculations. It was observed that the coordination number increases with increasing temperature. A possible reason for this behaviour could be segregation in the first shell as the temperature increases. The increase in temperature brings about separation of pairs of atoms leading to overcrowding in the first shell. The determination of the average interatomic distance in binary alloys is difficult to achieve and in the present investigation we endeavoured to determine the symmetric distance ratio  $r_{\max}/r_0$ . A value of 0.68 was obtained. This is less than the values obtained for individual metallic components [22]. Figure 4 shows the variation of the effective  $g(r_{\max})$  with the temperature. As the temperature increases, the main peak in the effective pair distribution function decreases in accordance with observed trends [23].

Table 3 shows the calculated dynamic coefficients from our studies. We have agreements of theory and calculated values; the diffusion coefficient increases with increasing temperature, while the viscosity decreases with increasing temperature. However, a breakdown in the calculated surface tension (not shown

Table 2. Calculated structural information of Fe-Mg alloys.

$T$ (K)	$C_n$	$r_0/\sigma_{\text{Fe-Mg}}$	$r_{\max}/\sigma_{\text{Fe-Mg}}$	$\frac{r_{\max}}{r_0}$	$g(r_{\max})$
1273	8.8	1.56	1.06	0.68	2.47
1373	8.9	1.56	1.06	0.68	2.41
1573	9.0	1.56	1.06	0.68	2.35

Table 3. Calculated diffusion coefficients and viscosity in Fe-Mg.

$T$ (K)	$D$ ( $10^{-9} \text{ m}^2 \text{ s}^{-1}$ )	$\eta$ (mPa) $\times 10$
1273	0.5759	93.0346
1373	0.6411	92.6909
1473	0.6689	92.3961
1573	0.7237	92.1402

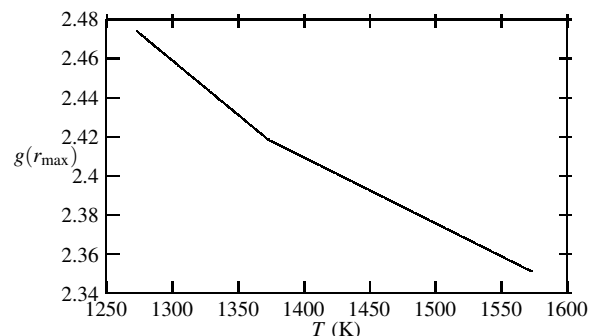


Fig. 4. Plot of the principal peaks in the effective pair distribution function for Fe-Mg alloy.

here) using both the diffusion coefficient and viscosity confirms our observation that segregation dominates the Fe-Mg alloy at the investigated temperatures.

#### 4. Conclusion

We have used the interatomic Lennard-Jones potential to determine the adhesion energy and surface traction in the binary liquid Fe-Mg alloy over the temperature range of 1273 K–1573 K. The adhesion energy of the liquid binary Fe-Mg alloy shows no temperature dependence. The calculated surface traction has a peak at 2.24 Å. The calculated structural and dynamical quantities favour segregation in the Fe-Mg binary alloy. It would be interesting, however, to investigate if the high pressure of the earth's interior will destroy segregation of species in Fe-Mg.

#### Acknowledgements

The authors are grateful to the Abdus Salam International Centre for Theoretical Physics (ICTP), Trieste, Italy, and the Swedish Agency for International Devel-

opments (SIDA) for hospitality and financial support under the Associateship Scheme of ICTP. G.A. A. ac-

knowledges book donation support from the German Academic Exchange Services (DAAD).

- [1] T.D. Yensen and N. A. Ziegler, *Trans. AIME* **95**, 313 (1931).
- [2] R. Kremann and J. Lorber, *Monatsh. Chem.* **35**, 608 (1914).
- [3] W. Bulian and E. Fahrenhorst, *Z. Metallkd.* **34**, 166 (1942).
- [4] A. Beerwald, *Z. Metallkd.* **33**, 28 (1941).
- [5] E. Fahrenhorst and W. Bulian, *Z. Metallkd.* **33**, 31 (1941).
- [6] G. Siebel, *Z. Metallkd.* **39**, 22 (1948).
- [7] D. W. Mitchell, *Trans. AIME* **175**, 570 (1948).
- [8] B. J. Keene, *Int. Mater. Rev.* **38**, 157 (1993).
- [9] I. Egry, S. Sauerland, and G. Jacobs, *High Temperature – High Pressure* **26**, 213 (1994).
- [10] I. Seyhan and I. Egry, *Int. Thermophys.* **20**, 1017 (1999).
- [11] F. Xiao, R. Yang, and C. Zhang, *Mater. Sci. and Engin. B* **132**, 183 (2006).
- [12] R. Novakovic, E. Ricci, D. Giuranno, and A. Passerone, *Surf. Sci.* **576**, 175 (2004).
- [13] L. Verlet, *Phys. Rev.* **159**, 98 (1967).
- [14] H. A. Steel, *The Interaction of Gases with Solid Surfaces*, Pergamon Press, Oxford 1974.
- [15] C. Kittel, *Introduction to Solid State Physics*, Wiley, New York 1975.
- [16] V. M. Muller, V. S. Yushchenko, and B. V. Derjaguin, *J. Colloid Interface Sci.* **77**, 91 (1981).
- [17] N. Yu and A. A. Poloycarpou, *J. Colloid Interface Sci.* **278**, 428 (2004).
- [18] J. N. Israelachvili, *Intermolecular and Surface Forces*, 2<sup>nd</sup> ed., Academic Press, San Diego 1992.
- [19] J. Ergy, G. Lohoefer, and S. Sauerland, *J. Non-Cryst. Solids* **156**, 830 (1993).
- [20] J. V. A. Butler, *Proc. R. Soc. A* **135**, 348 (1932).
- [21] D. Maugis, *J. Colloid Interface Sci.* **150**, 243 (1992).
- [22] Y. Waseda, *The Structure of Non-Crystalline Materials: Liquids and Amorphous Solids*, McGraw-Hill, New York 1980.
- [23] T. Iida and R. I. L. Guthrie, *The Physical Properties of Liquid Metals*, Clarendon Press, Oxford 1988.